Progress in Physics of Applied Materials 7 (2027), Serial Number 14, 65-74

Semnan University

Progress in Physics of Applied Materials

journal homepage: https://ppam.semnan.ac.ir/

# Photocurrent Performance of Copper (II) 2, 9, 16, 23-tetra-tert-butyl Phthalocyanine/Carbon Nanotube Active Layer Deposited on Silicon/Silicon Dioxide (Si/$SiO_2$) Substrate

**Baneen Jabar Abduljawad**[*], **Hikmat Adnan Banimuslem**

*Department of Physics, College of Science, University of Babylon, Babylon, Iraq*

**ARTICLE INFO**

Article history:
Received: 7 May 2026
Revised: 15 June 2026
Accepted: 20 June 2026
Published online: 17 August 2026

Keywords:
Phthalocyanine;
Multi-walled Carbon Nanotubes;
Composite materials;
Photocurrent;
Optical Absorption;
Quantum Efficiency;
Responsivity.

**ABSTRACT**

We synthesized and investigated a hybrid thin film composed of multi-walled carbon nanotubes (MWCNTs) and copper (II) 2,9,16,23-tetrabutylphthalocyanine (CuPc) to explore the influence of these interactions on the optical, electrical, and photoelectric properties. Improved charge transfer between CuPc moieties and CNT walls was observed in the ultraviolet and visible regions, where the optical absorption behavior of the hybrid material exhibited a redshift (indicative of longer wavelengths) and increased absorption intensity. CNTs provide numerous conductive pathways for charge carriers, thereby significantly improving the electrical conductivity of the hybrid material. Atomic Force Microscopy (AFM) results revealed that surface roughness and complexity increased upon the incorporation of CNTs into the CuPc film. This further confirms better contact between CuPc and CNTs, supporting the conclusion that the addition of CNTs has greatly altered the surface morphology of the pristine CuPc. Investigations of the hybrid material's photoelectric properties on a silicon oxide (Si/$SiO_2$) substrate demonstrated that, under illumination, the photocurrent exceeded the dark current, indicating an improved light response compared to pristine CuPc. All materials used in this research were obtained from Sigma-Aldrich. An electric potential, varying from -5 V to +5 V, was applied to the sample under various experimental conditions to determine the influence of voltage on the material's photoelectric and insulating responses. The light source used in this work was a 120-watt halogen lamp, with an irradiance of approximately 38.2 W/$m^2$ illuminating the sample. The light was focused on a rectangular sample area of 6 $cm^2$. Five replicates were conducted to confirm the accuracy of the results. This experiment was performed at approximately 25 °C and 30% humidity. The dark and light currents measured for CuPc and CuPc/MWCNT materials were $1.8\times10^{-6}$ A and $3.2\times10^{-6}$ A (dark current), and $2\times10^{-5}$ A and $9.8\times10^{-5}$ A (light current), respectively. Additionally, the data revealed a strong response to the addition of 10% MWCNT to the sample.

## 1. Introduction

The rapid development of nanotechnology has struggled to keep pace with growing technological demand, and a growing range of substances with unique mechanical, optical, or electrical characteristics has become essential to meet these requirements. Among the wide variety of hybrid materials, new technologies are emerging from the synergistic interaction of two or more efficient components [1,2]. Furthermore, research concerning the interaction of carbon nanotubes with conjugated molecules – mainly metal phthalocyanines (MPcs) – has begun to attract more interest over the last few decades as a new topic of fundamental research with potential applications ranging from sensing to photovoltaics [3]. Leveraging the excellent electrical, thermal, and mechanical properties of carbon nanotubes (CNTs), as well as the optoelectronic characteristics of

* Corresponding author.
*E-mail address:* benin.kadhim561@student.uobabylon.edu.iq

**Cite this article as:**

Abduljawad, B.J., Banimuslem, H,A., 2027. Photocurrent Performance of Copper (II) 2, 9, 16, 23-tetra-tert-butyl Phthalocyanine/Carbon Nanotube Active Layer Deposited on Silicon/Silicon Dioxide (Si/$SiO_2$) Substrate. *Progress in Physics of Applied Materials*, *7*(1), pp.65-74. DOI: 10.22075/ppam.2026.41075.1221

© 2026 The Author(s). Progress in Physics of Applied Materials published by Semnan University Press. This is an open access article under the CC-BY 4.0 license. (https://creativecommons.org/licenses/by/4.0/)

MPcs, is an ideal route to fabricate composite materials that can greatly enhance their relative responses compared to pristine CNTs. Phthalocyanines (Pcs) and their metallo-derivatives (MPc) generally represent a class of materials with pronounced potential for the fabrication of several nonlinear optical devices due to their optical limiter behavior, fast response time, peculiar electronic absorption features, and an extremely delocalized π- π conjugated electron system [4] . Another advantage of MPcs is that they can be processed in thin-film form and deposited by various techniques, including spin-coating, drop-casting, thermal evaporation, and Langmuir-Blodgett deposition. Substituted MPcs have also been utilized as an active membrane in surface plasmon resonance (SPR) and total internal reflection ellipsometry (TIRE) sensors [5,6].

MPcs are π-π-electron-conjugated macrocyclic compounds with excellent potential for applications in chemical and biosensors, liquid crystals, field-effect transistors, electrochromic devices, and data storage applications. Device performance is influenced by the structure of MPcs, which affects their physical attributes (such as specific surface area, electron-transfer characteristics, and thermal stability) [7]. The key advantages of MPcs over their organic analogs are: (i) A tunable structure, offering great flexibility in introducing different substituents to the periphery as well as in coordinating nearly every metallic element in the center of the macrocycle; (ii) An exceptional thermal and chemical stability compared to most molecular materials; (iii) The possibility to fabricate a large variety of thin films by distinct deposition methods [8].Although MPc-based devices have been studied for a long time, some specific limitations still need to be addressed, including: (1) improving the reproducibility of organic thin-film devices due to poor control over the crystallite orientation of polycrystalline MPc films; (2) enhancing the selectivity and sensitivity of MPc thin-film sensors; (3) providing more homogeneous films during the manufacturing of semiconductor devices, minimizing pin-holes that can lead to short-circuit issues; and (4) increasing charge carrier mobility in organic thin-film diodes or transistors, which is strongly determined by various factors such as the type, orientation, and structure of MPcs, together with their film thickness and the nature of the interface between the organic film and electrodes [9,10].In contrast, CNTs, which exhibit a high aspect ratio, are π-π-conjugated nanomaterials. This class of carbon materials exhibits numerous advantageous mechanical, thermal, and electrical properties; therefore, these carbon structures are excellent candidates for various applications, such as a reinforcing filler in polymers, a component of thermal management systems, and a substrate material for nanoelectronic devices [11,12]. CNTs are known to be highly sensitive to their surrounding chemical environment. The wide applications of CNTs can be attributed to their superior electrical properties, small size, extremely high surface-to-volume ratio, and strong adsorption capacity [13,14]. However, the low solubility and dispersibility of CNTs in common solvents have limited their use as active layers via facile methods such as spin-coating. Acid treatment and other modification methods, such as mixing with organic dyes, can also be used to address shortcomings in poorly dispersed CNTs. Another drawback is that CNTs are optically passive and very difficult to use as an active layer in photocurrent, photovoltaic, and optical detection methods, as well as in any application that requires light absorption [15]. In addition, the surface modification of CNTs through hybridization with MPcs can improve their photocurrent and photovoltaic performance due to π-π stacking interactions between CNTs and MPcs, which are more effective than either individual component alone [16-18].

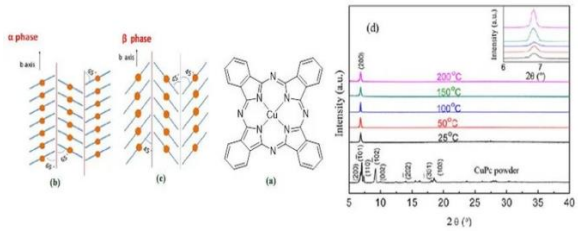


**Fig. 1.** (a) The CuPc molecular structure, (b) the layered architectures of -phase, (c) phase (d) X-ray diffraction (XRD) patterns of CuPc powders and films deposited at various temperatures on the substrate.

**Table 1.** Basic physicochemical properties of the materials used in this study.

| Parameter | Copper Phthalocyanine (CuPc) |
|---|---|
| Chemical Name | Copper(II) 2,9,16,23-tetra-tert-butyl-29H,31H-phthalocyanine |
| Abbreviation | CuPc $(tBu)_4$ |
| Molecular Formula | $C_{48}H_{48}CuN_8$ |
| Molecular Weight (g/mol) | 800.49 g/mol |
| Purity (%) | Dye content = 97% |
| Physical Appearance | Blue solid (blue pigment/solid) |
| Solubility | Organo-soluble / soluble in organic solvents |
| Supplier / Source | Aldrich (Sigma-Aldrich), Product No. 423165 |

This study focuses on the fabrication of CuPc/MWCNT hybrid thin films deposited on silicon/silicon dioxide ($Si/SiO_2$) substrates to investigate their photocurrent performance and conduct complementary characterizations, including optical absorption and morphological analysis.

The principal aim of the current study is to develop a nanocomposite material combining phthalocyanine with carbon nanotubes and to examine the correlation between its structure and enhanced photocurrent response. To achieve this goal, the following specific objectives were pursued: (i) synthesis of the nanocomposite and subsequent thin film preparation; (ii) investigation of the structural properties; (iii) characterization of the optical properties; (iv) analysis of the electrical properties; and finally, (v) utilization of the synthesized samples as an active layer for photocurrent applications.

## 2. Experimental Part

The hybrid materials CuPc and multi-walled carbon nanotubes (MWCNTs) were synthesized as described below. The substrate was rinsed with distilled water, then with laboratory-grade ethanol, to remove contaminants or impurities. The following is a flowchart of the work steps.

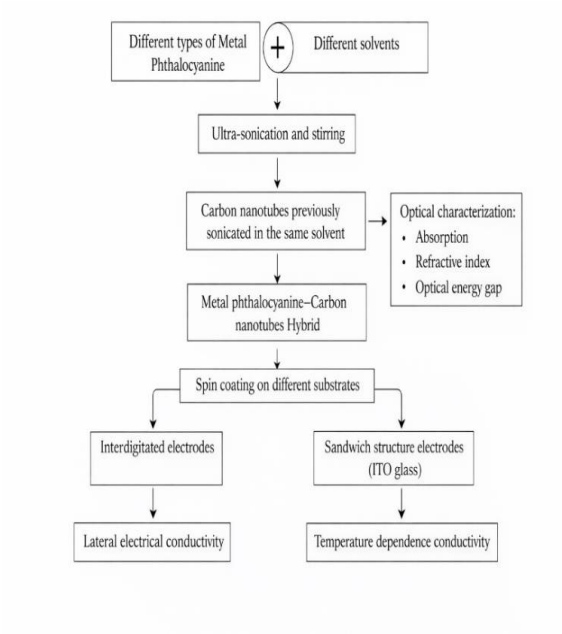


**Fig. 2.** Flowchart illustrating the preparation methodology and optical–electrical characterization of the metal phthalocyanine/CNT hybrid thin films.

Then, 10 mg of CuPc was accurately weighed and dissolved in 400 mL of dimethyl sulfoxide (DMSO). After stirring the mixture at room temperature for 30 min, the CuPc was completely dissolved. For the hybrid sample, 9 mg of CuPc was weighed and diluted in DMSO to a final volume of 300 mL, and the solution was stirred until complete dissolution. Then, 1 mg of MWCNTs was dispersed in 100 mL of DMSO and shaken for 30 min to ensure a homogeneous dispersion. To prepare hybrid materials containing 10 wt% MWCNTs in CuPc, a suspension of MWCNTs was added dropwise to the CuPc solution. The hybrid samples were sonicated for 30 min after preparation to ensure a uniform dispersion of CuPc and MWCNTs. Then, the samples were mechanically ground in a mechanical grinder for 15 min to improve the homogeneity of the CuPc/MWCNT mixture. The hybrid material was drop-cast on ITO-coated glass substrates for I–V measurements and on $Si/SiO_2$ substrates for photocurrent measurements. The drop-casting was performed using the drop-dry-drop technique to ensure complete coverage of the substrate. The deposited layer is a p-type semiconductor, as shown by Hall measurements. Silver paste was used to fabricate the electrodes, as shown in Figure 3, to provide good electrical contact with the active layer, ensure current flow, and form the top electrode. (See Figure 3 for clarity.) These conditions were repeated five times to assess reproducibility, yielding highly consistent results. The measurements were repeated five times for each sample, and the results clearly showed that the devices were highly reversible.

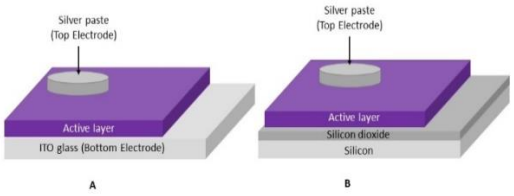


**Fig. 3.** The slides used in this work and their layers.

The optical properties of the samples were characterized by recording their absorption spectra in the UV and visible regions using UV–vis spectroscopy. I–V measurements and photocurrent characterization of the samples were carried out using a Keithley 2400 SourceMeter. The light source used in this work was a 120 W halogen lamp. The photocurrent experiment was conducted using a time-dependent program interfaced with the SourceMeter. The thickness of all prepared thin films was measured using an optical refractometer. All materials used in this work were supplied by Sigma-Aldrich and used without further purification.

## 3. Results and Discussion

### *3.1. Atomic Force Microscopy*

Fig. 4 presents the atomic force microscopy (AFM) images of (A) the CuPc thin film and (B) the CuPc/CNT film. This technique enables high-resolution analysis of surface morphology, including RMS roughness, growth orientation, and film uniformity, and is therefore useful for structural characterization, as AFM provides three-dimensional (3D) surface topography at high spatial resolution without requiring complex sample preparation [19].

From the images, the surface morphology of CuPc appears homogeneous and particle-like, with a surface roughness of approximately (Ra) 15.35 nm. Phthalocyanines and their metal derivatives tend to form homogeneous thin films on substrates by various processing methods [20]. Figure 4(B) shows the image of carbon nanotubes. CNTs typically increase film roughness because they are one-dimensional nanomaterials [21]. The roughness of the CuPc/CNT sample was measured to be 89.02 nm. This significant increase in roughness, compared to the pristine CuPc film, contributes to a larger effective surface area and enhances the interfacial contact between active materials. As shown in Figure 4, the RMS values were 22.5 nm and 106 nm for the CuPc and CuPc/CNT samples, respectively. The grain size was in the range of 280–380 nm. This increase in surface roughness of CuPc/MWCNT films significantly influences charge generation, transport, and collection. A coarser interfacial structure increases the effective surface area available for light absorption and facilitates exciton dissociation into free charge carriers. This enhanced surface morphology, in turn, improves charge percolation pathways, thereby reducing recombination losses and improving the collection efficiency of photogenerated electrons and holes at the electrodes. Consequently, a direct relationship

exists between the RMS roughness values of the CuPc/MWCNT films and the resulting photocurrent response and optoelectronic performance.

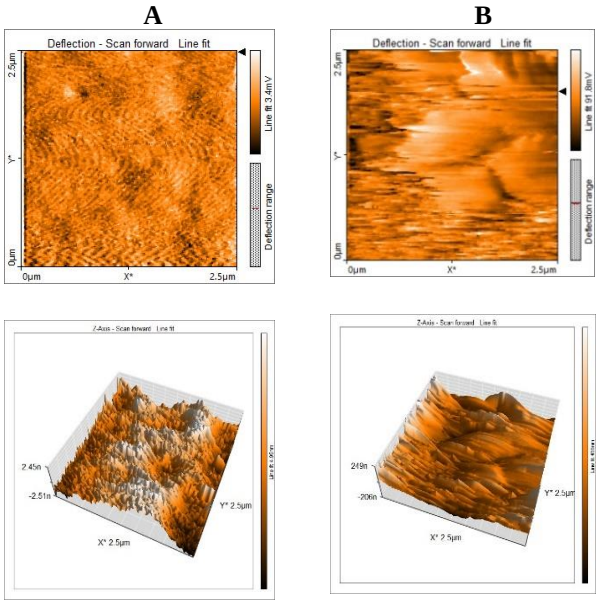


**Fig. 4.** Atomic force microscopy images of (A) CuPc and (B) CuPc/CNT thin films

### *3.2. UV-Visible Spectra*

The UV–Visible plots in Figure 5 show the optical absorption of copper phthalocyanine (CuPc) without and with carbon nanotubes. The black solid line is the pristine CuPc solution, and the purple dashed curve is the CuPc/CNT composite [22,23]. Both spectra show a typical absorption profile of phthalocyanine with two distinctive bands: the B-band in the near-UV-visibie ( ≈ 340 nm) and the Q-band at visible ( ≈ 670 nm ), from π → π * electronic transition within the conjugated macrocyclic core. Compared with pure CuPc, the CuPc–CNT spectrum shows a slight red shift in the Q-band position and a moderate increase in absorption intensity [22]. These spectral changes indicate the presence of π–π stacking interactions and the electronic coupling between the aromatic systems of CuPc molecules and the graphitic layers of CNTs. This coupling leads to charge delocalization and interfacial charge transfer, both of which contribute to the hybrid's improved optical activity [24,25]. See the Figure 5.

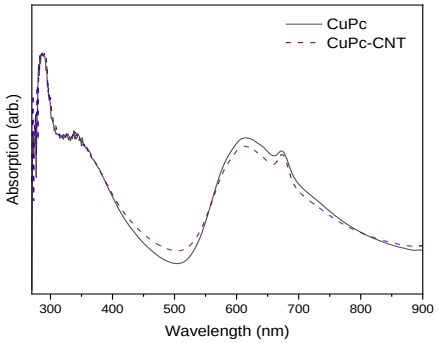


**Fig. 5.** UV–Vis absorption spectra of CuPc and CuPc/CNT solutions in DMSO.

Fig. 5 provides strong evidence of a decrease in transition energy, accompanied by increased conjugation and improved orbital overlap between the electronic levels of CuPc and CNTs. The increase in absorption intensity nevertheless indicates enhanced light-harvesting ability, making the CuPc–MWCNT hybrid more sensitive in the visible region. Overall, these modifications confirm that the CNTs are well incorporated into the CuPc network, thereby promoting the formation of an efficient, optically active nanohybrid material. Optical transmittance measurements of the prepared samples were performed over the 300–900 nm range to examine the effect of carbon nanotube addition on transparency [26]. The measured spectra exhibited two distinct transmission bands: the B-band in the near-UV region (330–380 nm) and the Q-band in the visible region (620–690 nm). These bands are directly assigned to the π→π* electronic transitions previously observed in the absorption spectra, thereby confirming the intrinsic molecular nature of the phthalocyanine macrocycle. In conclusion, the transmittance study confirmed that incorporating CNTs alters optical transparency and improves light-harvesting performance in the phthalocyanine systems examined, consistent with their absorption features. This suggests potential applications in optoelectronic materials [27,28].

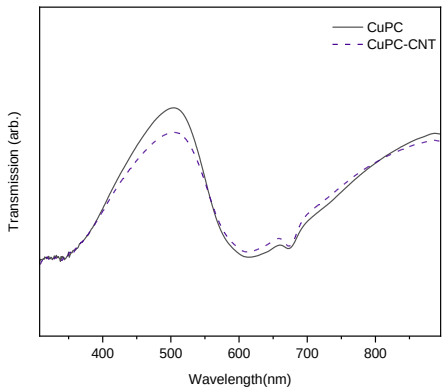


**Fig. 6.** Transmittance spectra of CuPc and CuPc/CNT solutions in DMSO.

Fig. 6 exhibited the transparency behavior of copper phthalocyanine (CuPc), and CuPc dispersed in a carbon nanotube (CNT) composite has been studied using optical transmittance spectra. The solid black curve represents the uncoated CuPc, which exhibits mediocre transmittance across the entire visible region. Two obvious bands are observed, corresponding to the characteristic B-band at around 340 nm and the Q-band at about 670 nm [29]. The π→π* transitions are responsible for these bands that appeared in the CuPc conjugated aromatic macrocycle. After introducing MWCNTs, the transmission of the CuPc/CNT composite declines slightly across the entire wavelength range and shifts slightly toward longer wavelengths for the main transmission features [30].

The optical reflectance of Pc dyes is well known and delivers valuable information on the electronic construction as well as the interface between the film surface and incident light [31]. Usually, metallo-phthalocyanines (MPcs) have low reflectance in the range of visible light due to their strong absorption in the π–π* transition band region. Figure 7 shows the reflectance spectra of CuPc and CuPc/MWCNTs hybrid solution. See the Figure 7.

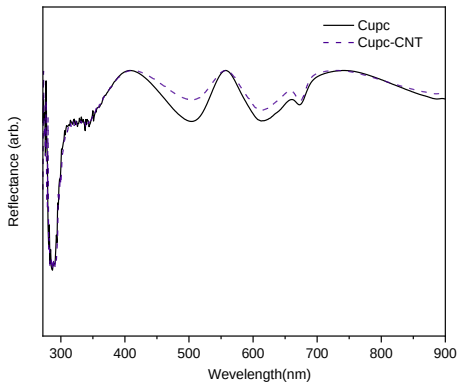


**Fig. 7.** Reflectance spectra of CuPc and CuPc/CNT solutions in DMSO.

Fig. 7 illustrates the reflectance spectra of CuPc and its CNT composite in the 300–900 nm range. The observed spectral variations indicate an optical effect resulting from the incorporation of carbon nanotubes [32]. The reflectance of pure CuPc (black solid line) is consistently low over the visible region, attributed to its pronounced absorption arising from strong π→π∗ transitions within the conjugated macrocyclic moiety. Several small reflection features are observed in the vicinity of the B-band (~340 nm) and Q-band (~670 nm), corresponding to characteristic molecular excitations of CuPc. Upon the introduction of carbon nanotubes (purple dashed line), the spectra exhibit a slight increase in integrated reflectance intensity in the 400–800 nm range, accompanied by a moderate smoothing of the spectral oscillations [33,34]. This behavior is attributed to changes in the material lattice and local refractive index induced by the CNTs, which provide additional light-scattering sites at the nanointerfaces between CuPc molecules and the CNT network. Consequently, a portion of the incident photons is redirected (scattered) by interfacial roughness and improved optical contact instead of undergoing pure absorption [35].

Fig. 8 presents the determination of the optical energy gap (Eg) of the prepared samples. As a fundamental parameter determining the electronic properties of semiconductors, the optical band gap dictates the absorption edge and material suitability for optoelectronic and photovoltaic applications [36]. The interaction between the π-electron systems of the CNTs and the phthalocyanine matrix induces significant changes in the energy gap. The extended conjugation of the CNTs and their high electrical conductivity facilitate charge transfer and orbital overlap with the phthalocyanine molecules, resulting in a slight reduction in the optical band gap. This reduction is primarily driven by the emergence of new electronic states at the Fermi level introduced by the CNTs, which promote electron delocalization across the CuPc/CNT interface. The Tauc equation, which explains the connection between the absorption coefficient and the photon energy, was utilized to determine the optical band gap [37]:

$$\alpha = A(hv - Eg)^{1/2}/hv \quad (1)$$

where α, Eg, and A stand for the absorption coefficient, band gap, and constant, respectively. The samples were liquid, and the cuvette thickness was 1 cm. The absorption coefficient was calculated according to the following equation [37]:

$$\alpha = \frac{2.303\ A}{t} \quad (2)$$

where A is the absorption and t is the thickness.

Phthalocyanine typically has two absorption regions: one in the visible and the other near UV. Figure 8 shows the energy gap calculated from the higher-absorption region near the UV.

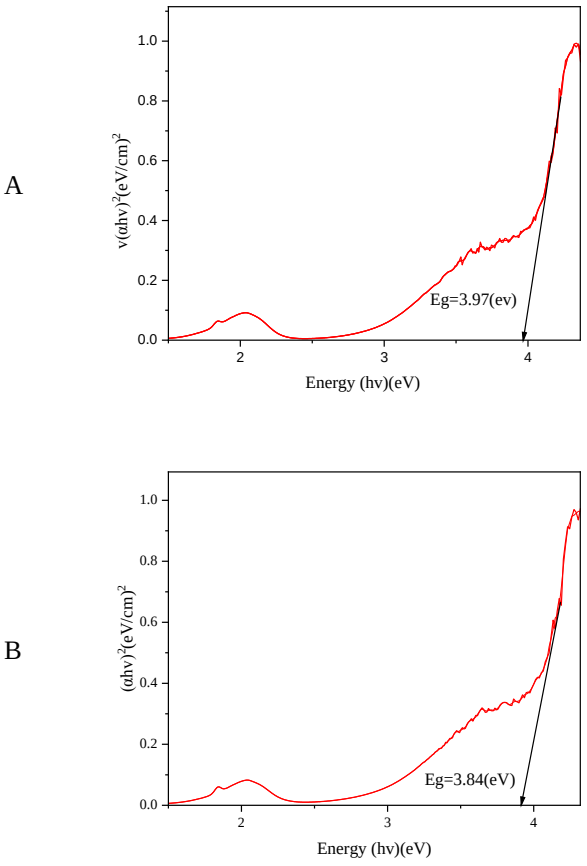


**Fig. 8.** Tauc plot of $(\alpha h\nu)^2$ versus photon energy (hν) for (A) the pure CuPc sample and (B) the CuPc/CNT hybrid sample.

The observed optical band gaps of 3.97eV and 3.84eV - much higher than typical bulk CuPc values (~1.7–2.0eV) but in line with sample thin-film nature and carbon nanotube integration (modifies local electronic structure). Moreover,

thin-film UV–Vis measurements are lower than those for bulk crystals because π–π* transitions in single molecules, rather than in complexes responsible for nonlinear optics within a single bulk crystal, lead to larger gaps.

The optical transition characteristics of pure copper phthalocyanine (CuPc) are demonstrated in Figure 8(A), wherein the band-to-band edge with an Eg ~ 3.97 eV was a direct allowed state. This relatively large band gap arises from the intrinsic electronic structure of the CuPc macrocyclic architecture, which features a stable π–π-conjugated system and exhibits weak intermolecular charge-carrier transport.

The large difference indicates a large excitation energy necessary for charge carriers to transfer from the valence band to the conduction band of pure CuPc. When the CuPc matrix is embedded with CNTs Figure 8(B), a relatively smaller band gap of 3.84 eV was observed. This slight decrease in Eg indicates the emergence of electronic coupling between the π orbitals of CuPc and the extended π electrons on the CNT. This coupling generates localized states within the forbidden energy region and further reduces the band gap. Whitmore, due to the conductive characteristics of carbon nanotubes, charge transfer among phthalocyanine chains is facilitated by increased orbital overlap and a lowered potential barrier resulting from electron excitation. As a consequence, the composite material exhibits a preferred charge-transport path and an enhanced optical response compared with the bare CuPc sample. This band-gap narrowing is a clear indication of π–π interactions and charge delocalization, thereby improving the optoelectronic properties of donors [38].

### *3.3. IV Measurements*

Fig. 9 represents the I-V characteristics of CuPc and CuPc/CNT thin films deposited on ITO glass as the bottom electrode, and the top electrode was silver, as represented in Figure 3(A). The conductivity was calculated from the fitting information in Figure 9 through the following equation [39]:

$$\sigma = \frac{d}{RA} \tag{3}$$

where σ is the conductivity measured in $\Omega^{-1}m^{-1}$, d is the film thickness, A is the cross-sectional area of the top electrode ($3.01 \times 10^{-9}$ $m^2$), and R is the resistance, which equals $slope^{-1}$[40].

$$\sigma = \frac{L}{RHWN_r} \tag{4}$$

where (H) is the thickness of the film equal (200,250), (L) is the space between fingers equal $10 \times 10^{-6}$μM, (W) is the electrode overlap distance equal 6.7mM, (Nr) is the number of fingers of interdigitated electrodes equal 100, and (R) is the resistance of the film.

These curves are quite useful because they indicate a material's behavior at different voltages by representing the relationship between current and applied voltage. See the Figure 9.

The conductivity values are represented in Table 2. The conductivity of CuPc/CNT is clearly higher than the conductivity of CuPc. The doping of organics with CNTs has been extensively studied due to the superior electrical and optical properties of CNTs. Specifically, CuPc is a viable option as a representative organic semiconductor for optoelectronic devices such as photodetectors [42]. The addition of CNTs, which have superior electrical conductivity and mechanical properties, could enhance the electrical behavior of organic materials for optoelectronics. When CNTs are mixed with CuPc, the resulting product exhibits higher electrical conductivity than pure CuPc [43,44]. This improvement is attributed to the conductive CNTs, which facilitate charge percolation through the hybrid material, thereby yielding a stronger linear response in its I-V characteristics. The addition of CNTs forms a conductive network that facilitates more efficient electron transfer, thereby increasing current density at the same voltage. This is consistent with reports in the literature, which show that adding CNTs to organic semiconductors can significantly increase electrical conductivity [45]. See the table (2).

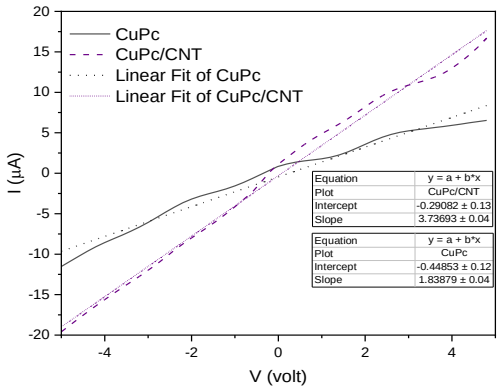


**Fig. 9.** Current-Voltage (I-V) Characteristics of CuPc and CuPc-CNT thin films deposited on ITO glass.

**Table 2.** Conductivities of CuPc and CuPc/CNT thin films.

| Sample | Slope (Fig.6) | R (Ω) | Film Thickness | Conductivity ($\Omega^{-1}M^{-1}$) |
|---|---|---|---|---|
| CuPc | $1.84\times10^{-6}$ | $5.4\times10^{5}$ | 200 nm | $1.2\times10^{-4}$ |
| CuPc/CNT | $3.74\times10^{-6}$ | $2.6\times10^{5}$ | 250 nm | $3.1\times10^{-4}$ |

### *3.4. Photocurrent (Photoconductivity)*

The photoresistive properties of the CuPc/CNT hybrid were studied to determine its light responsivity. The change in photoresistance was used to assess the impact of light on the material's electrical conduction behavior. The observation of an apparent photoresponse to light irradiation renders the material interesting for optical sensing [46]. Figure 10 represents the time dependence of the current response due to light radiation. From this figure, it is clear that the response is large in both samples, with and without carbon nanotubes. However, the CuPc sample was irreversible, whereas the CuPc/CNT sample was reversible and stable over time. This observation is attributed to the electron channel formed in the composite upon interaction between the phthalocyanine and the

carbon nanotube channel, which prevents electron penetration into the materials, leading to saturation and irreversibility in the CuPc sample. See the Figure 10.

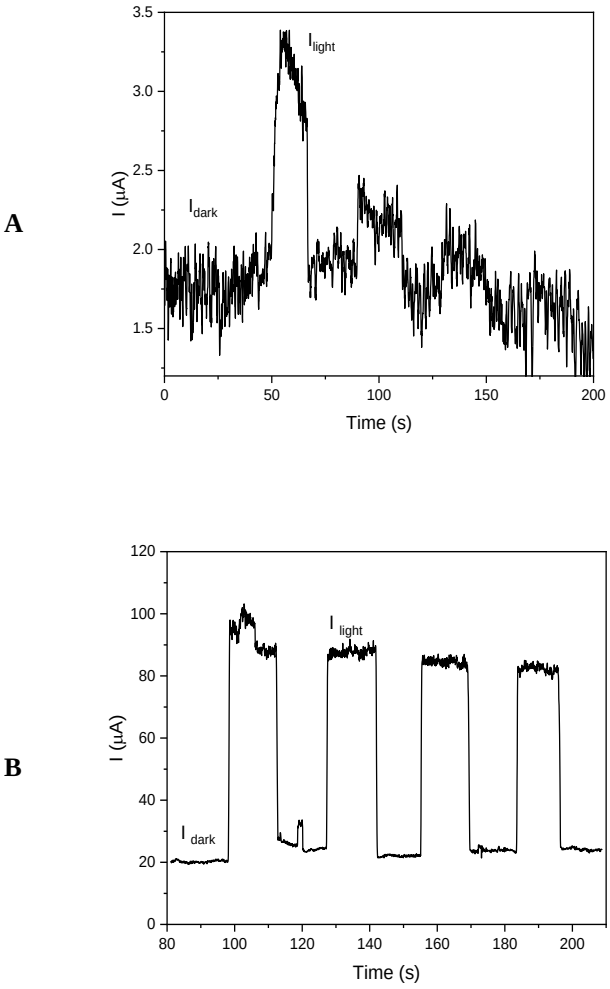


**Fig. 10.** Photoresistance (Photoconductivity) of (A) CuPc (B) CuPc-CNT Hybrid.

The photoresistivity and current response to light were calculated from the matching information included in Figure 10 using the following equations [47]:

$$I_{photo} = I_{light} - I_{dark} \quad (5)$$

where $I_{photo}$ is the photocurrent, $I_{light}$ is the current measured under illumination, and $I_{dark}$ is the dark current. This relationship immediately corresponds to the number of created carriers by absorption of a photon. The relative increase in the current due to illumination can be expressed in terms of the sensitivity of the material towards optical excitation, either photoresponse or sensitivity PS (%):

$$PS(\%) = \frac{I_{light} - I_{dark}}{I_{dark}} \times 100\% \quad (6)$$

This parameter provides a normalized measure of the material's response to incident radiation [48].

Another important parameter for characterizing photodetector performance is responsivity ($R_\lambda$) [49,50].

$$R_\lambda = \frac{I_{photo}}{P_{opt}} \quad (7)$$

where $P_{opt}$ is the incident optical power, a larger responsivity implies a better photon-to-current conversion.

The EQE (external quantum efficiency) characterizes how well incident photons are converted to charge carriers and is connected to responsivity by [51,52]:

$$EQE = \frac{hc}{q\lambda} R_\lambda \quad (8)$$

where h is the Planck constant, c is the speed of light, q is the elementary charge in coulombs, and λ is the wavelength of input light [53,54].

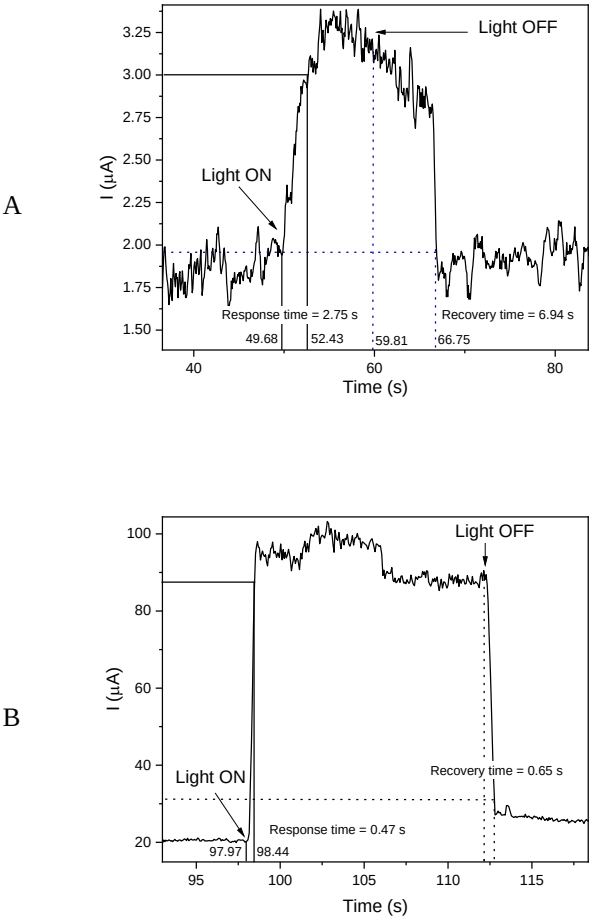


**Fig. 11.** The response and recovery times calculations for (A) CuPc and (B) CuPc/CNT.

Photogenerated current originates from photon absorption and subsequent electronic transitions, which are fundamental quantum phenomena. Upon photon incidence, electrons absorb discrete energy quanta and move from lower to higher energy levels. This excitation generates free charge carriers, thereby modulating electrical conductivity. The efficiency of this process is governed by incident photon energy, material morphology, and charge transport kinetics [55]. The dynamic characteristics of the photodetector are defined

by its response and recovery times. Response time is the interval required to reach 90% of the steady-state photocurrent upon illumination, and recovery time is the time required to decay to 10% of the peak value after the light source is removed. These parameters characterize the rates of carrier generation and recombination [56,57].

Fig. 11 illustrates the determination of these response and recovery times, while Table 3 summarizes the computed values. See the table (3) Photoconductive and photoresponse parameters of CuPc and CuPc–CNT photodetectors.

**Table 3.** Photoconductive and photoresponse parameters of CuPc and CuPc–CNT photodetectors.

| PARAMETERS | CuPc | CuPc -CNT |
|---|---|---|
| $I_{DARK}$(μA) | 1.9 | 20.5 |
| $I_{LIGHT}$(μA) | 3.2 | 87.2 |
| $I_{PHOTO}$(μA) | 1.3 | 66.7 |
| RESPONSE % | 68% | 325% |
| RESPONSIVITY(A/W) | $1.08 \times 10^{-6}$ | $5.55 \times 10^{-6}$ |
| EXTERNAL QUANTUM EFFICIENCY(EQE) | $2.31 \times 10^{-6}$ | $1.18 \times 10^{-6}$ |
| RESPONSE TIME (S) | 2.75 | 6.94 |
| RECOVERY TIME (S) | 0.47 | 0.65 |

The observed decrease in the external quantum efficiency (EQE) for the CuPc/CNT composite, despite the enhancement in photocurrent, can be attributed to increased non-radiative recombination pathways introduced by the incorporation of carbon nanotubes. Although CNTs significantly improve charge transport and electrical conductivity by providing efficient percolation networks, their presence may also introduce interfacial defect states and localized trap centers at the CuPc–CNT interface. These trap states can act as recombination sites, reducing the probability of successful photon-to-carrier conversion. Consequently, a fraction of the photogenerated charge carriers undergo recombination before contributing to the external circuit, leading to a reduction in the calculated EQE value. This behavior indicates that the improvement in photocurrent is mainly governed by enhanced carrier mobility and transport efficiency, whereas EQE is additionally sensitive to recombination dynamics and interfacial quality within the hybrid structure [58].

## 4. Conclusions

The optical and electrical properties of the composite are largely improved by the well combination of carbon nanotubes (CNTs) and copper phthalocyanine. The red-shifted absorption edge and higher extinction coefficient of the hybrid composite are attributed to electronic interactions between copper phthalocyanine (CuPc) and the nanotube walls, thereby increasing its potential for photonic materials and sensing applications and enhancing light absorption in the visible and ultraviolet ranges. The optical energy gap decreased from 3.97 eV to 3.84 eV after adding carbon nanotubes to the pure thallocyanine sample. The photoresistive characterizations also show that the response of the CuPc/CNT to 120 halogen illumination is much higher than that of pristine CuPc. This indicates enhanced electrical conductivity and photoresponse, which is beneficial for highly efficient photodetector and solar cell-type device applications. Additional CNT-induced charge-transfer pathways are responsible for the significantly enhanced photoresponse. These pathways promote efficient electron–hole separation under light irradiation, resulting in faster response times and higher sensitivity in photonic sensing applications. The response increased from 68% to 325% after the addition of carbon nanotubes. In addition, these results are consistent with the AFM measurements, indicating that CNT doping can substantially alter the surface morphology of CuPc thin films, thereby facilitating interfacial contact and charge transfer. These morphological changes support the enhanced roles of the CuPc/CNT composite in optical absorption, electrical conductivity, and photoresponse.

## Author Contributions

Baneen Jabar Abduljawad: Conceptualization, methodology, investigation, data analysis, writing – original draft.
Hikmat Adnan Banimuslem: Supervision, validation, formal analysis, review and editing.

## Funding Statement

The authors did not receive any funding for this work.

## Conflicts of Interest

The authors declare no conflicts of interest.

## Acknolegment

The authors would like to acknowledge the University of Babylon, College of Science, Department of Physics, for providing the necessary facilities and technical support to complete this work.

## References

[1] Banimuslem, H., Hassan, A., Basova, T., & Gürek, A.G. 2015. Copper Phthalocyanine Functionalized Single-Walled Carbon Nanotubes: Thin Films for Optical Detection. *Journal of Nanoscience and Nanotechnology*, 15(3), pp.2157-2167.

[2] Banimuslem, H., Hassan, A., Basova, T., & Ahsen, V. 2014. Copper Phthalocyanine/SWCNT Hybrid Thin Films for Pentachlorophenol Detection. *Sensors and Actuators B: Chemical*, 190, pp.990-998.

[3] Tuncel, S., Kaya, E.N., Basova, T., Banimuslem, H., Hassan, A., Gürek, A.G., & Ahsen, V. 2014. Effect of Pyrene Substitution on the Formation and Sensor Properties of Phthalocyanine-Single-Walled Carbon Nanotube Hybrids. *Sensors and Actuators B: Chemical*, 199, pp.277-283.

[4] Banimuslem, H., Hassan, A., Basova, T., & Gülmez, A.D. 2014. Copper Phthalocyanine/Single-Walled Carbon Nanotubes

Hybrid Thin Films for Pentachlorophenol Detection. *Sensors Actuators B: Chemical*, 190, pp.990-998.

[5] Wang, Y., Hu, N., Zhou, Z., Xu, D., Wang, Z., Yang, Z., Wei, H., Kong, E.S., & Zhang, Y. 2011. Single-Walled Carbon Nanotube/Cobalt Phthalocyanine Derivative Hybrid Material: Preparation, Characterization, and Its Gas Sensing Properties. *Journal of Materials Chemistry*, 21(8), pp.3779-3787.

[6] Tuncel, S., Basova, T., Hassan, A., & Gürek, A.G. 2012. Liquid Crystalline Octasubstituted Lead(II) Phthalocyanines: Effects of Alkoxy and Alkylthio Substituents on Film Alignment and Electrical Properties. *New Journal of Chemistry*, 36(7), pp.1665-1672.

[7] Basova, T., Jushina, I., Gürek, A.G., & Ahsen, V. 2009. Investigation of Gas-Sensing Properties of Copper Phthalocyanine Films. *Materials Science and Engineering C*, 29(6), pp.814-818.

[8] Wang, S. Y., Xu, J. H., Yang, W. Y., Chen, Y., & Yang, Y. J. 2013. Preparation and Gas Sensing Properties of 2, 9, 16, 23-Tetra-Tert-Butyl-29H, 31H-Copper (II) Phthalocyanine LB Thin Films. *Advanced Materials Research*, 622, pp.679-684.

[9] Belakhmima, R. A., Dkhireche, N., Touir, R., & Touhami, M. E. 2015. Development of a multi-component SG with CTAB as corrosion, scale, and microorganism inhibitor for cooling water systems. *Materials Chemistry and Physics*, 152, pp.85-94.

[10] Tan, Y., Zu, J., & Zhang, Z. 2015. Design and development of a miniature multi-degree-of-freedom in-plane motor using iron–gallium alloy. *Sensors and Actuators A: Physical*, 236, pp.140-149.

[11] McEvoy, T. M., Long, J. W., Smith, T. J., & Stevenson, K. J. 2006. Nanoscale conductivity mapping of hybrid nanoarchitectures: Ultrathin poly (o-phenylenediamine) on mesoporous manganese oxide ambigels. *Langmuir*, *22*(10), pp.4462-4466.

[12] Jafari, M. J., Azim-Araghi, M. E., Barhemat, S., & Riyazi, S. 2012. Effect of post-deposition annealing on surface morphology and gas sensing properties of palladium phthalocyanine thin films. *Surface and interface analysis*, 44(5), pp.601-608.

[13] Li, J., Lu, Y., Ye, Q., Cinke, M., Han, J., & Meyyappan, M. 2003. Carbon nanotube sensors for gas and organic vapor detection. *Nano letters*, 3(7), pp.929-933.

[14] Aydın, M., Alıcı, E. H., Bilgicli, A. T., Yarasir, M. N., & Arabaci, G. 2017. Synthesis, characterization, aggregation, fluorescence and antioxidant properties of bearing (4-(methylthio) phenylthio) tetra substituted phthalocyanines. *Inorganica Chimica Acta*, 464, pp.1-10.

[15] Shamsipoor, A. S., Bagheri-Mohagheghi, M. M., & Mokaripoor, E. 2022. Structural, electrical and optical properties of SnO2: B transparent semiconducting thin films. *Progress in Physics of Applied Materials*, 2(1), pp.1-10.

[16] Peter, Y. U., & Cardona, M. (2010). *Fundamentals of semiconductors: physics and materials properties*. Springer Science & Business Media.

[17] Abbas, N. K., Abdulameer, A. F., Ali, R. M., & Alwash, S. M. 2019. The effect of heat treatment on optical properties of copper (II) phthalocyanine tetrasulfonic acid tetrasodium salt (CuPcTs) organic thin films. *Silicon*, 11(2), pp.843-855.

[18] Singh, A., Uddin, M. A., Sudarshan, T., & Koley, G. 2014. Tunable reverse-biased graphene/silicon heterojunction schottky diode sensor. *Small*, 10(8), pp.1555-1565.

[19] Bube, R. 2012. *Electronic properties of crystalline solids: an introduction to fundamentals*. Elsevier.

[20] Matsumoto, N., Shima, H., Fujii, T., & Kannari, F. 1997. Organic electroluminescence cells based on thin films deposited by ultraviolet laser ablation. *Applied physics letters*, 71(17), pp.2469-2471.

[21] Bottari, G., de la Torre, G., Guldi, D. M., & Torres, T. 2010. Covalent and noncovalent phthalocyanine− carbon nanostructure systems: synthesis, photoinduced electron transfer, and application to molecular photovoltaics. *Chemical reviews*, 110(11), pp.6768-6816.

[22] El Nhass, M. M., Soliman, H. S., Metwally, H. S., Farid, A. M., Farag, A. A. M., & El Shazly, A. A. 2001. Optical properties of evaporated iron phthalocyanine (FePc) thin films. *Journal of Optics*, 30(3), pp.121-129.

[23] Pankove, J. I. 2012. *Optical processes in semiconductors*. Courier Corporation.

[24] Singh, Y. 2013. Electrical resistivity measurements: a review. In *International journal of modern physics: Conference series* (Vol. 22, pp. 745-756). World Scientific Publishing Company.

[25] Raïssi, M., Leroy-Lhez, S., & Ratier, B. 2016. Enhanced photocurrent and stability of organic solar cells using solution-based TS-CuPc interfacial layer. *Organic Electronics*, 37, pp.183-189.

[26] Rajesh, K. R., & Menon, C. S. 2005. Electrical and optical properties of vacuum deposited MnPc thin films. *The European Physical Journal B-Condensed Matter and Complex Systems*, 47(2), pp.171-176.

[27] Sánchez-Vergara, M. E., Guevara-Martínez, E., Arreola-Castillo, A., & Mendoza-Sevilla, A. 2019. Fabrication of hybrid membranes containing nylon-11 and organic semiconductor particles with potential applications in molecular electronics. *Polymers*, 12(1), p.9.

[28] Banimuslem, H. A. 2015. *Organic/carbon nanotubes hybrid thin films for chemical detection*. Sheffield Hallam University (United Kingdom).

[29] He, N., Chen, Y., Bai, J., Wang, J., Blau, W. J., & Zhu, J. 2009. Preparation and optical limiting properties of multiwalled carbon nanotubes with π-conjugated metal-free phthalocyanine moieties. *The Journal of Physical Chemistry C*, 113(30), pp.13029-13035.

[30] Matsumoto, S., Matsuhama, K., & Mizuguchi, J. 1999. β Metal-free phthalocyanine. *Crystal Structure Communications*, 55(1), pp.131-133.

[31] Serebrennikova, S. I., Kopylova, D. S., Gladush, Y. G., Krasnikov, D. V., Mailis, S., & Nasibulin, A. G. 2023. Photogating interfacial effects in carbon nanotube-based transistors on a Si/SiO 2 substrate toward highly sensitive photodetection. *Nanoscale*, 15(47), pp.19351-19358.

[32] Darwish, S., El Zawawi, I. K., & Riad, A. S. 2005. Photovoltaic properties of ZnSe/metal-free phthalocyanine

heterojunctions deposited on substrates of InP single crystals. *Thin Solid Films*, 485(1-2), pp.182-187.

[33] Somani, P. R., & Radhakrishnan, S. J. M. C. 2003. Electrochromic materials and devices: present and future. *Materials chemistry and physics*, 77(1), pp.117-133.

[34] Schütze, A., Pieper, N., & Zacheja, J. 1995. Quantitative ozone measurement using a phthalocyanine thin-film sensor and dynamic signal evaluation. *Sensors and Actuators B: Chemical*, 23(2-3), pp.215-217.

[35] He, N., Chen, Y., Bai, J., Wang, J., Blau, W. J., & Zhu, J. 2009. Preparation and optical limiting properties of multiwalled carbon nanotubes with π-conjugated metal-free phthalocyanine moieties. *The Journal of Physical Chemistry C*, 113(30), pp.13029-13035.

[36] Niazov-Elkan, A., Weissman, H., Dutta, S., Cohen, S. R., Iron, M. A., Pinkas, I., ... & Rybtchinski, B. 2018. Self-assembled hybrid materials based on organic nanocrystals and carbon nanotubes. *Advanced Materials*, 30(2), p.1705027.

[37] Kumar, A. K. S., Zhang, Y., Li, D., & Compton, R. G. 2020. A mini-review: How reliable is the drop casting technique?. *Electrochemistry Communications*, 121, p.106867.

[38] Karl, N. 2003. Charge carrier transport in organic semiconductors. *Synthetic metals*, *133*, pp.649-657.

[39] Sze S.M., Ng K.K. 2006. Physics of Semiconductor Devices. *Wiley*, 3rd Edition.

[40] Bube, R. H. 1992. *Photoelectronic properties of semiconductors*. Cambridge University Press.

[41] Kymakis, E., & Amaratunga, G. A. J. 2002. Single-wall carbon nanotube/conjugated polymer photovoltaic devices. *Applied Physics Letters*, 80(1), pp.112-114.

[42] Lakowicz, J. R. (Ed.). 2006. *Principles of fluorescence spectroscopy*. Boston, MA: springer US.

[43] Knox, R. S. 1963. Theory of excitons, Acad. *Press, NY*.

[44] Qi, T., Yu, Y., Liu, J., Jia, Y., & Ding, D. (2022, August). Enhanced performance of single-walled carbon nanotube-germanium near-infrared photodetector by doping with Au nanoparticles. In *Photonics* (Vol. 9, No. 9, p. 615). MDPI.

[45] Sönmez, M., Berber, İ., & Akbaş, E. 2006. Synthesis, antibacterial and antifungal activity of some new pyridazinone metal complexes. *European Journal of Medicinal Chemistry*, 41(1), pp.101-105.

[46] Ban, K., Nishizawa, K., Ohta, K., van de Craats, A. M., Warman, J. M., Yamamoto, I., & Shirai, H. 2001. Discotic liquid crystals of transition metal complexes 29: Part 28: Ref. 1. mesomorphism and charge transport properties of alkylthio-substituted phthalocyanine rare-earth metal sandwich complexes Elemental analysis data, recrystallization solvents, yields and optical absorption spectral data for [(CnS) 8Pc] 2M are available as supplementary data. For direct electronic access see http://www. rsc. org/suppdata/jm/b0/b003984p. *Journal of Materials Chemistry*, 11(2), pp.321-331.

[47] Barranco, A., Borras, A., Gonzalez-Elipe, A. R., & Palmero, A. 2016. Perspectives on oblique angle deposition of thin films: From fundamentals to devices. *Progress in Materials Science*, 76, pp.59-153.

[48] Capista, D., Lozzi, L., Pelella, A., Di Bartolomeo, A., Giubileo, F., & Passacantando, M. 2023. Spatially resolved photo-response of a carbon nanotube/Si photodetector. *Nanomaterials*, 13(4), p.650.

[49] Hernández, A., Sánchez, J. G., Ortiz, J., Martinez-Ferrero, E., Palomares, E., & Sastre-Santos, Á. 2025. Tri-tert-butyl arylamine zinc phthalocyanine derivatives as p-type self-assembled molecules for efficient perovskite solar cells. *Journal of Materials Chemistry C*, 13(31), pp.15977-15987.

[50] Koshiba, Y., Sugimoto, I., Horike, S., Fukushima, T., & Ishida, K. 2023. Fabrication and local electrical characterization of p–n junction copper phthalocyanine nanorods. *physica status solidi (a)*, 220(24), p.2300243.

[51] Zhang, Q., Li, M., Li, L., Geng, D., Chen, W., & Hu, W. 2024. Recent progress in emerging two-dimensional organic–inorganic van der Waals heterojunctions. *Chemical Society Reviews*, 53(6), pp.3096-3133.

[52] Stenzel, O. 2005. *The physics of thin film optical spectra: an introduction*. Berlin, Heidelberg: Springer Berlin Heidelberg.

[53] Rana, A., Park, S. Y., Labanti, C., Fang, F., Yun, S., Dong, Y., ... & Durrant, J. R. 2024. Octupole moment driven free charge generation in partially chlorinated subphthalocyanine for planar heterojunction organic photodetectors. *Nature Communications*, 15(1), p.5058.

[54] Vergara, M. E. S., Plata, E. I. S., Indili, R. B., Salcedo, R., & Toledano, C. Á. 2024. Structural determination, characterization and computational studies of doped semiconductors base silicon phthalocyanine dihydroxide and dienynoic acids. *Heliyon*, 10(3).

[55] Soncini, C., Costantini, R., Dell'Angela, M., Morgante, A., & Pedio, M. 2025. Interfacial Charge Transfer Enhances Transient Surface Photovoltage in Hybrid Heterojunctions. *Nanomaterials*, 15(3), p.154.

[56] Thyda, L., Joseph, J. K., Koppula, N., Sana, S., & Kuppusamy, T. 2025. Carbon Quantum Dots/ZnO Hybrid Nanostructured Thin Films and UV Photodetector Performances. *physica status solidi (a)*, 222(18), p.2500458.

[57] Tsuneda, T., & Taketsugu, T. 2023. Roles of Singlet Fission in the Photosensitization of Silicon Phthalocyanine. *The Journal of Physical Chemistry Letters*, 14(51), pp.11587-11596.

[58] Wang, Y., Deng, W., Shi, X., Ren, X., Li, B., Li, Y., ... & Zhang, X. 2025. Molecule upgrading metal-semiconductor buried contacts for high-performance and high-ideality single-crystal organic thin-film transistors. *National Science Review*, 12(7), p.nwaf207.

.